Journal of Inorganic and General Chemistry
ZAAC
Zeitschrift für anorganische und allgemeine Chemie
www.zaac.wiley-vch.de
RESEARCH ARTICLE
Check for updates
DOI: 10.1002/zaac.202300100

Synthesis and Crystal Structures of Three Thioether Functionalized Lithium Silylamides

Phil Liebing,[a] Philipp Schatz,[a] and Kurt Merzweiler*[a]

Dedicated to Prof. Wolfgang Weigand on the Occasion of his 65th birthday

A series of three lithium silylamides $Li_2Me_2Si(NC_6H_4\text{-}2\text{-}SR)_2$ (R = Me, Ph, ^{t}Bu) were prepared from the reaction of the corresponding silylamines $Me_2Si(NH\text{-}C_6H_4\text{-}2\text{-}SR)_2$ with *n*-butyl lithium. X-ray single crystal structure analyses revealed the formation of dimers $[Li_4\{Me_2Si(NC_6H_4\text{-}2\text{-}SR)_2\}_2]$ with $Si_2N_4Li_4$ hetero-adamantane cores. Recrystallisation of $[Li_4\{Me_2Si(NC_6H_4\text{-}2\text{-}SMe)_2\}_2]$ and $[Li_4\{Me_2Si(NC_6H_4\text{-}2\text{-}SPh)_2\}_2]$ from diethyl ether led to the formation of the adducts $[Li_4(Et_2O)_2\{Me_2Si(NC_6H_4\text{-}2\text{-}SMe)_2\}_2]$ and $[Li_4(Et_2O)\{Me_2Si(NC_6H_4\text{-}2\text{-}SPh)_2\}_2]$. In the case of the SMe derivative the addition of two diethyl ether molecules led to a rearrangement of the $Si_2N_4Li_4$ core to give a double decker structure and in contrast the hetero adamantane structure is retained in the diethyl ether adduct of the SPh derivative.

Introduction

Silylamides $R_2Si(NR')_2^{2-}$ are versatile ligands that have been used with great success in main group and transition metal chemistry.[1] Moreover, the coordination properties of the silyamide ligands can be tuned by the introduction of side arm donor groups. This has been shown as early as 2004 by Passareli *et al.* who used OR and NR_2 functionalized silylamides for the generation of catalytically active zirconium complexes.[2] In our recent studies we are interested in the properties of thioether functionalized silylamides $R_2Si(NC_6H_4\text{-}2\text{-}SR')_2^{2-}$ (R = Me, Ph; R' = Me, Ph, ^{t}Bu). Previous work has shown that thioether functionalized derivatives are suitable starting materials for the generation of coinage metal complexes like $[M_2\{Me_2Si(NC_6H_4\text{-}2\text{-}SPh)_2\}(PMe_3)_2]$ (M = Cu,[3] Ag, Au[4]). Furthermore Ni(II) complexes of the type $[Ni\{R_2Si(NC_6H_4\text{-}2\text{-}SR')_2\}]$[5] and Mo(II) compounds of the type $[Mo_2\{R_2Si(NC_6H_4\text{-}2\text{-}SR')_2\}_2]$ were studied.[6] Usually, the synthesis of these complexes is achieved by a metathesis reaction between the appropriate metal halide, acetate or acetylacetonate with the lithiated silylamine $Li_2R_2Si(NC_6H_4\text{-}2\text{-}SR')_2$. In most cases, the isolation of the extremely air and moisture sensitive lithium silylamides is not required and further reactions can be done from *in situ* generated products. However, there are several x-ray structure determinations on lithiated aminosilanes. The first dates back to the year 1986, when Brauer et al. reported on $Li_2Me_2Si(N^tBu)_2$.[7] In the following years $Li_2Me_2Si(NMes)_2$ (1991),[8] $Li_2(THF)_3Me_2Si(N^tBu)_2$ (1998),[9] $Li_2Me_2Si(NDipp)_2$ (2002),[10] $Li_2Me_2Si(NCHMePh)_2$ (2005),[11] $Li_2Ph_2Si(N^tBu)_2$ (2014)[12] and $Li_2Me_2Si(N^iPr)_2$ (2020)[13] were reported. Additionally, there are some rare crystal structure determinations on silylamides bearing N donor groups, like 8-quinolyl,[14] (di-isopropylamino)ethyl and (dimethyllamino)ethyl.[15] In this report we would like to shed some light on the properties of the thioether functionalized silyamides, particularly on their crystal structures.

Results and Discussion

The aminosilanes $Me_2Si(NH\text{-}C_6H_4\text{-}2\text{-}SMe)_2$ (**1**), $Me_2Si(NH\text{-}C_6H_4\text{-}2\text{-}SPh)_2$ (**2**) and $Me_2Si(NH\text{-}C_6H_4\text{-}2\text{-}S^tBu)_2$ (**3**) were prepared according to a previously reported procedure from Me_2SiCl_2 and the lithium amides $LiNH(C_6H_4\text{-}2\text{-}SMe)$, $LiNH(C_6H_4\text{-}2\text{-}SPh)$ and $LiNH(C_6H_4\text{-}2\text{-}S^tBu)$.[4,16,5] Treatment of the aminosilanes **1**–**3** with *n*-butyllithium in *n*-hexane as solvent led to the precipitation of $Li_2Me_2Si(NC_6H_4\text{-}2\text{-}SMe)_2$ (**4**), $Li_2Me_2Si(NC_6H_4\text{-}2\text{-}SPh)_2$ (**5**) and $Li_2Me_2Si(NC_6H_4\text{-}2\text{-}S^tBu)_2$ (**6**) as colorless solids in nearly quantitative yield (Scheme 1). Compounds **4**–**6** are soluble in toluene, diethyl ether and THF and much less soluble in *n*-hexane. On contact with air and moisture the silylamides are rapidly decomposed.

The ^{29}Si-NMR spectra of compounds **4**–**6** consist of singlet signals with chemical shifts δ = −20.4, −21.9 and −24.8 ppm, respectively (Table 1). In comparison with the corresponding aminosilanes $Me_2Si(NH\text{-}C_6H_4\text{-}2\text{-}SR)_2$ these signals are shifted by 10.4–13.5 pm to higher field. Contrary to this the ^{1}H-NMR signals of the Me_2Si groups (0.37, 0.02, 0.01 ppm) display a marginal downfield shift compared to the parent aminosilanes

[a] Dr. P. Liebing, P. Schatz, Prof. Dr. K. Merzweiler
Institut für Chemie
Naturwissenschaftliche Fakultät II
Universität Halle
Kurt-Mothes-Str. 2, 06120 Halle, Germany
and
Current address: Friedrich-Schiller-Universität Jena
Institute of Inorganic and Analytical Chemistry
Humboldtstr. 8, 07743 Jena, Germany
E-mail: kurt.merzweiler@chemie.uni-halle.de

Journal of Inorganic and General Chemistry
ZAAC
Zeitschrift für anorganische und allgemeine Chemie

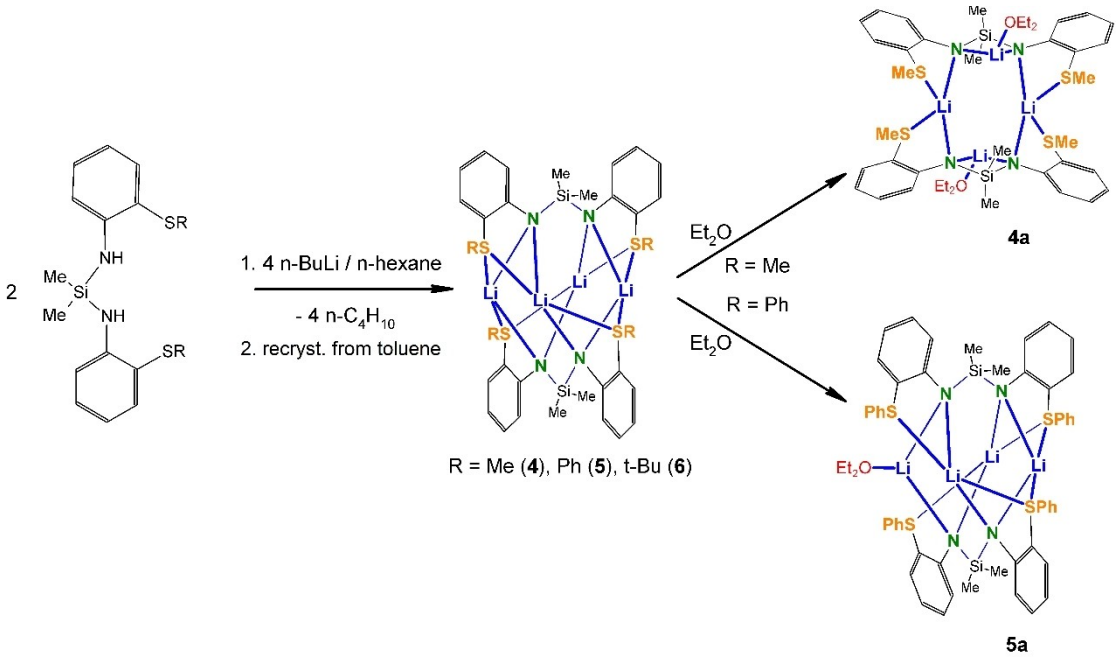

Scheme 1. Synthesis of the lithium silylamide compounds **4**–**6**.

Table 1. ^{29}Si NMR shifts of compounds **4**–**6** and related aminosilanes **1**–**3**.

compound	δ ^{29}Si /ppm	compound	δ ^{29}Si /ppm
$Li_2Me_2Si(NC_6H_4\text{-}2\text{-}SMe)_2$ (**4**)	−20.4	$Me_2Si(NH\text{-}C_6H_4\text{-}2\text{-}SMe)_2$ (**1**)	−10.0[4]
$Li_2Me_2Si(NC_6H_4\text{-}2\text{-}SPh)_2$ (**5**)	−21.9	$Me_2Si(NH\text{-}C_6H_4\text{-}2\text{-}SPh)_2$ (**2**)	−10.2[16]
$Li_2Me_2Si(NC_6H_4\text{-}2\text{-}S^tBu)_2$ (**6**)	−24.8	$Me_2Si(NH\text{-}C_6H_42\text{-}S^tBu)_2$ (**3**)	−11.3[5]

(0.27, −0.05, −1.6 ppm). The same holds for the SMe signal in compound **4** (2.08 ppm) and the S^{t}Bu signal in compound **6** (1.29 ppm) which display downfield shifts of 0.08–1.2 ppm.

Compounds **4**–**6** were recrystallized from toluene solutions to give $[Li_4\{Me_2Si(NC_6H_4\text{-}2\text{-}SMe)_2\}_2]\cdot 0.5$ toluene, $[Li_4\{Me_2Si(NC_6H_4\text{-}2\text{-}SPh)_2\}_2]\cdot 4$ toluene and $Li_4\{Me_2Si(NC_6H_4\text{-}2\text{-}S^tBu)_2\}_2]$. In order to investigate the influence of coordinating solvents, compounds **4**–**6** were additionally crystallized from diethyl ether. Compounds **4** and **5** afforded the solvates $[Li_4(Et_2O)_2\{Me_2Si(NC_6H_4\text{-}2\text{-}SMe)_2\}_2]$ (**4 a**) and $[Li_4(Et_2O)\{Me_2Si(NC_6H_4\text{-}2\text{-}SPh)_2\}_2]$ (**5 a**). In the case of compound **6**, no diethyl ether solvate was formed.

Crystal structures

In order to gain more insight into the molecular structures of **4**–**6**, X-ray crystal structure determinations were carried out. Details of the crystallographic data are summarized in table 2. The molecular structures of the ether-free compounds **4**–**6** are closely related. The structures are best described starting from a nearly quadratic arrangement of four lithium atoms. This Li_4 square is capped by two μ_4-κ-N,N,N',N' silylamide units at the bottom and the top side. Both the silylamide units are mutually rotated by 90° with respect to the Si–Si' axis. In an alternative description, the $Si_2Li_4N_4$ cores may be considered as heteroadamantane cages with the nitrogen atoms at bridgehead positions (Figures 1–3).

Compound **4** crystallizes in the triclinic space group $P\bar{1}$ with two formula units of the lithium silylamide and one disordered toluene molecule per unit cell. The crystal structure consists of well separated molecules without any unusual short intermolecular contacts. The silylamide units exhibit no special crystallographic symmetry. However, the molecules are nearly C_2 symmetric with respect to the Si1–Si2 axis. Neglecting the small deviations of the $Si(NC_6H_4\text{-}SMe)_2$ units from planarity, the idealized molecular symmetry would be C_{2v}. Within the $Si_2N_4Li_4$ adamantane core the Li–N distances are 198.1(3)–201.9(3) pm and the Si–N distances range from 173.3(1) to 174.0(1) pm. The observed Li–N distances are quite typical for lithium silylamides and similar values have been reported for related compounds. Some representative examples are: $Li_2Me_2Si(N^tBu)_2$ 200.3–212.7 pm,[7] $Li_2Me_2Si(NDipp)_2$ (188.4–222.3 pm),[10] $Li_2Ph_2Si(N^tBu)_2$ (205.4–215.8 pm).[12] Apart from the amide nitrogen atoms, the coordination sphere of each lithium atom is completed by two neighboring SMe groups with Li–S separations of 245.4(3)–255.1(3) pm. These distances are in accordance with the observations in other lithium thioether complexes. Generally, Li–S distances can vary over a broad range. A search in the

Table 2. Crystallographic data and details of the crystal structure refinement for compounds **4**, **6**, **4a** and **5a**.

Compound	**4**	**5**	**6**	**4a**	**5a**
Empirical formula	$C_{32}H_{39}Li_4N_4S_4Si_2{\cdot}0.5\ C_7H_8$	$C_{52}H_{48}Li_4N_4S_4Si_2\ 4\ C_7H_8$	$C_{44}H_{64}Li_4N_4S_4Si_2$	$C_{40}H_{60}Li_4N_4O_2S_4Si_2$	$C_{56}H_{58}Li_4N_4OS_4Si_2$
Formula weight	738.42	941.12	861.17	841.10	1015.24
Temperature/K	170(2)	170(2)	170(2)	213(2)	200(2)
Wavelength/pm	71.073	71.073	71.073	71.073	71.073
Crystal system	triclinic	tetragonal	tetragonal	triclinic	monoclinic
Space group	$P\bar{1}$	$I4_1/a$	$P\bar{4}2_1c$	$P\bar{1}$	$P2_1/n$
Unit cell dimensions/pm/°	a = 1266.84(7)	1559.76(2)	1435.53(3)	955.44(4)	1243.71(6)
	b = 1352.56(7)	1559.76(2)	1435.53(3)	1128.17(5)	2594.2(1)
	c = 1352.32(8)	2903.44(5)	1159.40(2)	1284.63(6)	1937.47(9)
	α = 74.247(4)	90	90	112.286(3)	90
	β = 73.198(5)	90	90	109.440(4)	105.868(4)
	γ = 61.867(4)	90	90	93.252(4)	90
Volume/pm^3	$1930.9(2)\times10^6$	$7063.6(2)\times10^6$	$2389.2(1)\times10^6$	$1181.4(1)\times10^6$	$6012.8(5)\times10^6$
Z	2	4	2	1	4
Calculated density/g·cm^{-3}	1.270	1.232	1.197	1.182	1.122
Absorption coefficient/mm^{-1}	0.339	0.22	0.283	0.288	0.236
Crystal size/mm^3	0.45×0.30×0.30	0.5×0.30×0.25	0.35×0.35×0.30	0.46×0.40×0.28	0.40×0.28×0.28
Θ range for data collection/°	2.533–29.165	2.319–29.249	2.838–29.257	1.855–24.999	3.908 to 24.998
Reflections collected/unique	23064, 10369	33228/4755	22130, 3219	9364, 4145	26636, 10531
R(int)	0.0405	0.0490	0.0409	0.0592	0.0388
Refinement method	Full-matrix least-squares on F^2				
Data/restraints/parameters	10369/4/463	4755/0/161	3219/0/136	4145/0/259	10531/0/645
Goodness-of-fit on F^2	1.146	1.032	1.045	1.046	1.032
R_1 ($I > 2\sigma(I)$)	0.0384	0.0360	0.0289	0.0480	0.0403
wR_2 (all data)	0.1069	0.1057	0.0789	0.1384	0.1009
Diffractometer	Stoe IPDS 2	Stoe IPDS 2T	Stoe IPDS 2	Stoe IPDS 2	STOE IPDS 2T
CCDC	2260935	2260936	2260937	2260938	2260939

Cambridge Structural Database (CSD) revealed 77 Li–S-(thioether) distances in the range of 232.9–296.4 pm with a median value of 255.2 pm (lower quantile: 249.8 pm, upper quantile: 262.8 pm).[17]

Compound **5** crystallizes in the tetragonal space group $I4_1/a$. The crystal structure contains discrete $Li_4\{Me_2Si(NC_6H_4\text{-}2\text{-}SPh)_2\}_2$ molecules that exhibit crystallographically imposed $\bar{4}$ symmetry. The asymmetric unit consists of one quarter of the $Li_4\{Me_2Si(NC_6H_4\text{-}2\text{-}SPh)_2\}_2$ molecule that is situated around the *4a* position (1/2, 1/4, 3/8) with the silicon atom at the *8e* position (0, 1/4, z + 1/4). Additionally, the crystal structure contains one disordered toluene molecule in the asymmetric unit. The Li–N (200.3(2), 202.1(2) pm) and the Si–N distances (173.9(1) pm) are directly comparable with those of the prototype **4**. The most important difference arises from the markedly enlarged Li–S distances that are now 263.9(2) pm and 279.2(2) pm. This hints for a much weaker Li–S interaction as it is to be expected for the less electron donating SPh groups.

Compound **6** also belongs to the tetragonal system and crystallizes in the space group $P\bar{4}2_1c$. The unit cell contains two discrete molecules $Li_4\{Me_2Si(NC_6H_4\text{-}2\text{-}S^tBu)_2\}_2$. Like in the case of compound **5** one quarter of the $Li_4\{Me_2Si(NC_6H_4\text{-}2\text{-}S^tBu)_2\}_2$ molecule is placed around a special position with $\bar{4}$ site symmetry (*2a* at 1/2, 1/2, 1/2) and the silicon is at a *4c* position (1/2, 1/2, z) with C_2 site symmetry. The Li–N (199.0(4) and 199.3(4) pm) and the Si–N distances (173.7(2) pm) fit well to the observations in compounds **4** and **5**. However, unlike the previously mentioned compounds, the lithium atoms are tricoordinated and only one thioether group is bound to the LiN_2 unit. It may be assumed, that the decrease in coordination number is mostly due to the bulkiness of the *t*-Bu groups. The sum of the N–Li–N (128.1(2)°) and N–Li–S angles (87.3(1)°, 119.3(2)°) is 334.7° and indicates pyramidal coordination.

Crystallization of **4** from diethyl ether afforded the adduct $[Li_4(Et_2O)_2\{Me_2Si(NC_6H_4\text{-}2\text{-}SMe)_2\}_2]$ (**4a**). Compound **4a** crystallizes in the triclinic space group $P\bar{1}$. The crystal structure consists of discrete molecules that exhibit no unusual short contacts. Unlike compounds **4–6** the $Si_2Li_4N_4$ core displays a structure that is best described as double decker consisting of two SiN_2Li four-membered rings which are connected by two lithium atoms (Figure 4). The double decker cage is situated around a crystallographic center of inversion and thus possesses $\bar{1}$ symmetry. There are now two different coordination modes for the lithium atoms: Li1 is connected to two amide N atoms (N1 and N2) and additionally it bears one diethyl ether molecule. The coordination sphere of Li2 consists of the nitrogen atoms N2 and $N1^i$ along with the thioether sulfur atoms S2 and $S1^i$.

Crystallization of compound **5** from diethyl ether resulted in the formation of the complex $[Li_4(Et_2O)\{Me_2Si(NC_6H_4\text{-}2\text{-}SPh)_2\}_2]$ (**5a**). **5a** crystallizes in the monoclinic space group $P2_1/n$ with one formula unit in the asymmetric unit. The crystal structure exhibits discrete molecules $[Li_4(Et_2O)\{Me_2Si(NC_6H_4\text{-}2\text{-}SPh)_2\}_2]$ without any unusual short intermolecular contacts (Figure 5). The molecular structure is closely related to that of the starting compound **5**. The main difference results from the coordination

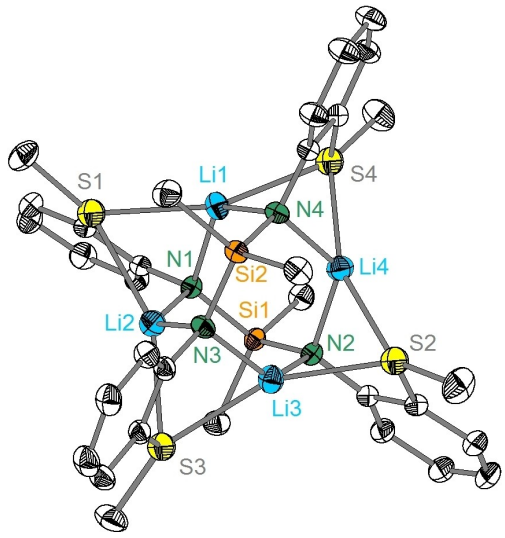

Figure 1. Molecular structure of compound **4** in the solid state. Thermal ellipsoids are shown at the 50 % probability level, H atoms are omitted for clarity. Selected bond lengths (pm) and angles (°): Li(1)–N(1) 201.9(3), Li(1)–N(4) 200.9(3), Li(2)–N(1) 200.4(3), Li(2)–N(3) 201.9(3), Li(3)–N(2) 198.1(3), Li(3)–N(3) 198.7(3), Li(4)–N(2) 199.3(3), Li(4)–N(4) 201.9(3), Li(1)–S(1) 248.8(3), Li(1)–S(4) 252.5(3), Li(2)–S(1) 249.6(3), Li(2)–S(3) 246.1(3), Li(3)–S(2) 251.6(3), Li(3)–S(3) 255.1(3), Li(4)–S(2) 254.1(3), Li(4)–S(4) 245.4(3), Si(1)–N(1) 173.9(1), Si(1)–N(2) 173.3(1), Si(2)–N(3) 173.9(1), Si(2)–N(4) 174.0(1), N(1)–Si(1)–N(2) 107.3(1), N(2)–Si(2)–N(3) 106.2(1), Li(1)–N(1)–Li(2) 84.4(1), Li(3)–N-(2)–Li(4) 86.1(1), Li(2)–N(3)–Li(3) 83.9(1), Li(1)–N(4)–Li(4) 86.2(1), N(1)–Li(1)–N(4) 122.8(2), N(1)–Li(2)–N(3) 124.2(2), N(2)–Li(3)–N(3) 127.5(2), N(2)–Li(4)–N(4) 123.3(2).

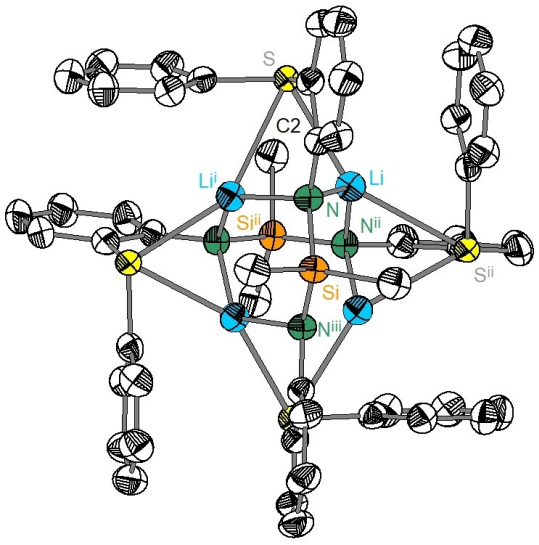

Figure 2. Molecular structure of compound **5** in the solid state. Thermal ellipsoids are shown at the 50 % probability level, H atoms are omitted for clarity. Selected bond lengths (pm) and angles (°): Li–N 200.3(2), Li-N^{ii} 202.1(2), Li–S 263.9(2), Li-S^{ii} 279.2(2), Si–N 173.9(1), Si-N^{iii} 173.9(1), N–Li-N^{ii} 127.3(1), N–Li-S 81.1(1), N–Li-S^{ii} 108.1(1), S–Li-S^{ii} 149.4(1), Li–S-Li^{ii} 57.8(1), N–Si-N^{iii} 104.9(1), Li–N-Li^{i} 81.6(1), Si-N–Li 121.0(1), Si–N-Li^{i} 110.2(1), C(2)–N–Si 120.4(1), C(2)–N–Li 104.9(1), C(2)–N–Li^{i} 112.1(1). Symmetry operators: i: −y + 3/4, x−1/4, −z + 3/4; ii: y + 1/4, −x + 3/4, −z + 3/4, iii: −x + 1, −y + 1/2, z.

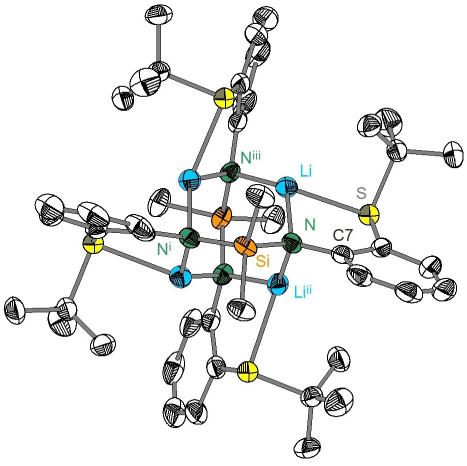

Figure 3. Molecular structure of compound **6** in the solid state. Thermal ellipsoids are shown at the 50 % probability level, H atoms are omitted for clarity. Selected bond lengths (pm) and angles (°): Li–N 199.3(4), Li–N^{iii} 199.0(4), Li–S 245.4(3), Si–N 173.7(2), Si–N^{i} 173.7(2), N–Li-N^{iii} 128.1(2), N–Li-S 87.3(1), N^{iii}-Li–S 119.3(2), Li–N-Li^{ii} 81.5(1), Si-N–Li 117.1(1), Si–N-Li^{ii} 114.9(1), C(7)–N–Si 121.5 (1), C(7)–N–Li^{ii} 102.8(2). Symmetry operators: i: −x + 1, −y + 1, z, ii: y, −x + 1, −z + 1, iii: −y + 1, x, −z + 1.

of one diethyl ether molecule to the lithium atom Li1. Unlike compound **4a** the $Si_2N_4Li_4$ adamantane skeleton is retained.

A comparison of the structural parameters of compounds **4**, **4a**, **5** and **5a** reveals that the influence of the diethyl ether coordination is rather complex. In the case of compound **4a** the most striking effect concerns the strong increase of the Li–S distances for diethyl ether coordinated lithium atom Li1. The Li1–S1 (314 pm) and Li1–S2 (320 pm) separations are around 67 pm larger than the average Li–S distances in compound **4**. This clearly indicates that the weakly coordinating thioether groups are easily displaced from the lithium coordination sphere by the stronger diethyl ether donor. This can be rationalized by Pearson's hard and soft acid and base (HSAB) concept.[18] For the lithium atom Li2 that bears no diethyl ether ligand, the Li–S separations (254.8(4) and 257.0(4)) are only marginally enlarged as compared with the average Li–S distance (250.4 pm) in compound **4**. In the case of compound **5a** the coordination of one diethyl ether molecule at the lithium atom Li1 has comparable consequences like in compound **4a**. In particular, the Li1–S1 (312 pm) and Li1–S2 (306 pm) distances are increased by around 38 pm with respect to the average Li–S separation in compound **5**. On the other hand, the Li2-S1 and Li4-S4 interactions are markedly strengthened as indicated by Li–S separations of 249.0(4) and 245.2(4) pm that are around 25 pm shorter than the average Li–S distances in compound **5**. A similar shortening is also observed for the Li3–S2 (252.6(4) pm) and Li4–S2 (249.2(4) pm)

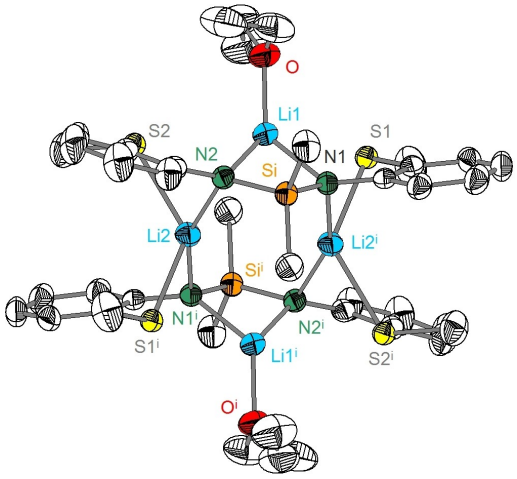

Figure 4. Molecular structure of compound **4a** in the solid state. Thermal ellipsoids are shown at the 50% probability level, H atoms are omitted for clarity. Selected bond lengths (pm) and angles (°): Li(1)–N(1) 203.0(4), Li(1)–N(2) 202.7(4), Li(1)–O 190.7(4), Li(2)–N(2) 202.4(4), Li(2)–N(1)^{i} 203.7(4), Li(2)–S(1)^{i} 254.8(4), Li(2)–S(2) 257.0(4), Si–N(1) 172.3(2), Si–N(2) 172.(2), N(1)–Li(1)–N(2) 80.0(2), O–Li(1)–N-(1) 129.1(2), O–Li(1)–N(2) 125.9(2), N(2)–Li(2)–N(1)^{i} 152.8(2), N(2)–Li-(2)–S(1)^{i} 114.6(2), N(2)–Li(2)–S(2) 76.4(1), N(1)^{i}-Li(2)–S(1)^{i} 75.7(1), S(1)^{i}-Li(2)–S(2)127.7(2), N(1)^{i} -Li(2)–S(2) 118.6(2), N(2)–Si–N(1) 98.4(1). Symmetry operator: i: −x, −y, -z+1.

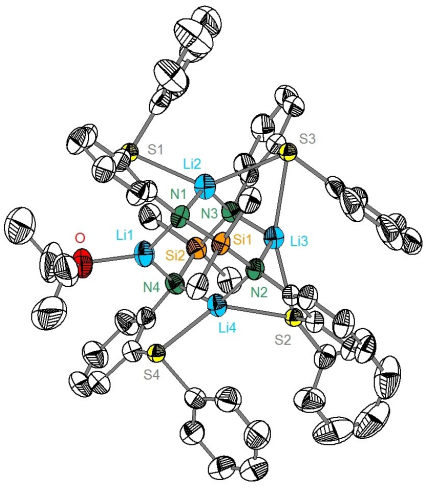

Figure 5. Molecular structure of compound **5a** in the solid state. Thermal ellipsoids are shown at the 50% probability level, H atoms are omitted for clarity. Selected bond lengths (pm) and angles (°) Li(1)–N(1) 204.1(4), Li(1)–N(4) 205.5(4), Li(2)–N(1) 197.9(4), Li(2)–N(3) 199.7(4), Li(3)–N(3) 200.9(4), Li(3)–N(2) 202.1(4), Li(4)–N(2) 203.3(4), Li(4)–N(4) 198.7(4), Li(1)–O 190.6(4), Li(2)–S(1) 249.0(4), Li(2)–S(3) 271.0(4), Li(3)–S(2) 252.6(4), Li(3)–S(3) 262.9(4), Li(4)–S(2) 249.2(4), Li(4)–S(4) 245.2(4), Si(1)–N(1) 173.6(2), Si(1)–N(2) 173.7(2), Si(2)–N(4) 173.1(2), Si(2)–N(3) 173.6(2), N(1)–Li(1)–N(4) 120.50(19), O–Li(1)–N-(1) 118.4(2), O–Li(1)–N(4) 120.9(2), N(1)–Li(2)–N(3) 130.6(2), N(1)–Li-(2)–S(1) 85.3(1), N(3)–Li(2)–S(1) 116.5(2), N(1)–Li(2)–S(3) 118.8(2), N(3)–Li(2)–S(3) 79.3(1), S(1)–Li(2)–S(3) 133.3(2), N(3)–Li(3)–N(2) 124.4(2), N(3)–Li(3)–S(2) 113.1(2), N(2)–Li(3)–S(2) 76.2(1), N(3)–Li-(3)–S(3) 81.2(1), N(2)–Li(3)–S(3) 111.7(2), S(2)–Li(3)–S(3) 156.9(2), N(4)–Li(4)–N(2) 129.5(2), N(4)–Li(4)–S(4) 86.3(1), N(2)–Li(4)–S(4) 122.1(2), N(4)–Li(4)–S(2) 113.4(2), N(2)–Li(4)–S(2) 76.8(1), S(4)–Li-(4)–S(2) 135.3(2), N(1)–Si(1)–N(2) 105.9(1), N(3)–Si(2)–N(4) 106.1(1).

distances while the Li2–S3 (271.0(4) pm) and Li3–S3 (262.9(4) pm) distances remain nearly unchanged.

In order to get some insight into the relative stability of the double decker structure **4a** vs. hypothetical adamantane structures, DFT calculations for **4a** and two adamantane type isomers (**4b** and **4c**) were carried out.

Figure 6 displays the DFT optimized structures of compound **4a** and the hypothetical **4b** and **4c** hetero-adamantane structures at the B3LYP/def2tzvp level of theory. All three structures are local minima as shown by the absence of imaginary vibrational frequencies. The geometrical parameters of the calculated structure of **4a** are in good agreement with the data from X-ray diffraction. The Li–N distances are slightly overestimated with 203.5–204.1 pm in the four-membered SiN_2Li rings and 205.8–206.4 pm for the bridging Li atoms. The same holds for the Li–O distance (196.8 pm) and the Li–S distances (258.4–259.5 pm). The calculated electronic energy for the **4a** isomer (−4132.251407 Hartree) is about 28.3 kJ/mol lower than for the **4b** isomer (−4132.240621 Hartree) and 54.7 kJ/mol for the **4c** variant (−4132.2306 Hartree). This clearly hints for the thermodynamically preferred formation of the double decker structure **4a**.

Conclusions

Three lithium silylamides of the type $Li_2Me_2Si(NC_6H_4\text{-}2\text{-}SR)_2$ with R = Me, Ph, ^{t}Bu were synthesized from the corresponding aminosilanes $Me_2Si(NH\text{-}C_6H_4\text{-}2\text{-}SR)_2$ and *n*-butyl lithium in *n*-hexane. In the solid state, the lithium silylamides exist as dimers $Li_4\{Me_2Si(NC_6H_4\text{-}2\text{-}SR)_2\}_2$ with $Li_4Si_2N_4$ hetero-adamantane cores as characteristic structural motif. Moreover, each of the structures displays an individual pattern for the intramolecular coordination of the SR groups depending on the thioether donor properties and steric requirements. On treatment with diethyl ether, compounds **4–6** behave differently. The formation of the bis diethyl ether adduct **4a** is accompanied by a structural rearrangement leading to a double decker structure while in the adduct **5a** the $Li_4Si_2S_4$ hetero-adamantane core is retained. Obviously, the reaction of compound **6** with diethyl ether is prevented by steric reasons. In future investigations, the work will be extended towards sodium and potassium derivatives of the thioether functionalized silylamines.

Experimental

General

All operations were performed under an argon atmosphere using standard Schlenk techniques. Diethyl ether, THF and toluene were distilled from sodium/benzophenone, *n*-pentane and *n*-hexane from lithium alanate. THF-D_8 was distilled from a sodium/potassium alloy under argon. ^{1}H-, ^{13}C-, and ^{29}Si-NMR spectra were recorded on a VARIAN Inova 500 (500 MHz) spectrometer. The IR spectra were

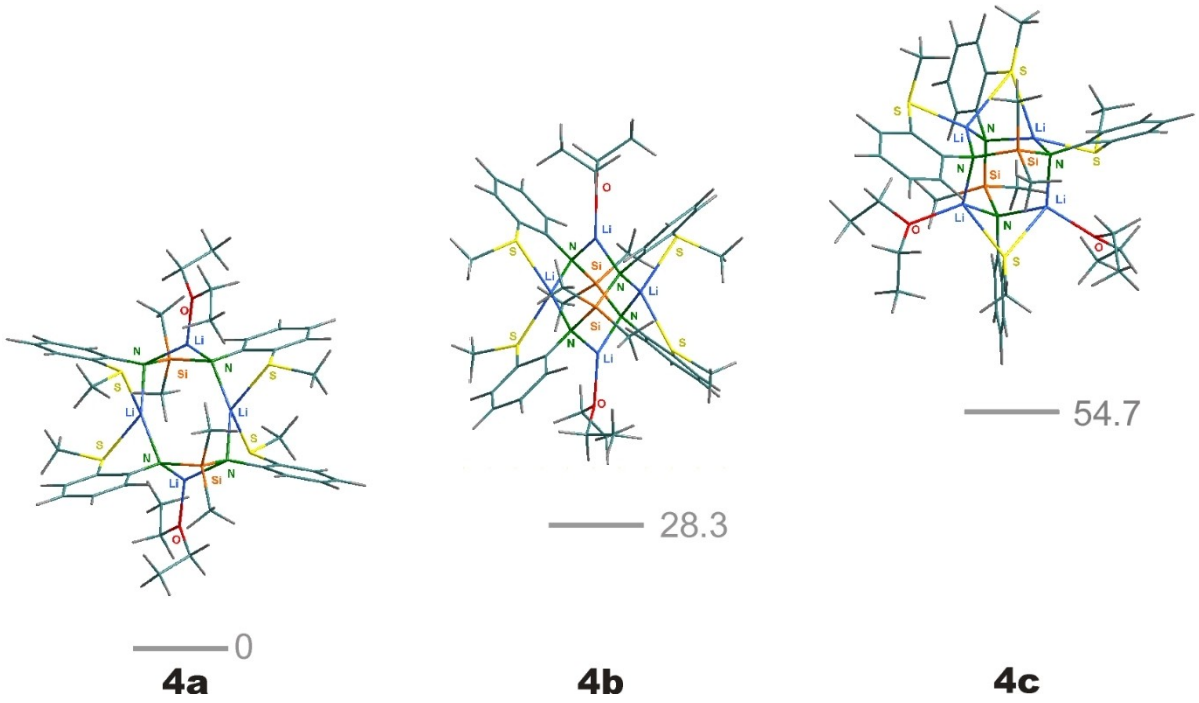

Figure 6. Graphical representation of the DFT optimized structures of **4a** and the hypothetical isomers **4b** and **4c**. The numbers denote the relative energies in kJ/mol.

measured with a BRUKER Tensor 27 spectrometer equipped with a diamond ATR unit. Due to the enhanced air and moisture sensitivity of compounds **4**–**6**, elemental analyses were not suitable. The analytical characterization was done by acidimetric titration after hydrolysis of the silylamides.

The aminosilanes $Me_2Si(NH\text{-}C_6H_4\text{-}2\text{-}SMe)_2$,[4] $Me_2Si(NH\text{-}C_6H_4\text{-}2\text{-}SPh)_2$[16] and $Me_2Si(NH\text{-}C_6H_4\text{-}2\text{-}S^tBu)_2$[5] were prepared according to previously published procedures.

Preparation of the lithium silylamides

In a typical experiment a solution or suspension of 5 mmol of the aminosilane $Me_2Si(NH\text{-}C_6H_4\text{-}2\text{-}SR)_2$ (R = Me, Ph) in 30 ml of *n*-hexane was treated with 6.3 ml of a 1.6 m solution of *n*-butyl lithium (10 mmol) in *n*-hexane at −80 °C. In the case of $Me_2Si(NH\text{-}C_6H_4\text{-}2\text{-}S^tBu)_2$ 1.7 mmol of the aminosilane and 3.4 mmol of *n*-BuLi were used. After warming up to room temperature the reaction mixture was refluxed for one hour and afterwards cooled down to room temperature. The colorless precipitates of the lithium silylamides were filtered off, washed with few ml of *n*-pentane and then dried in vacuum. $Li_2Me_2Si(NC_6H_4\text{-}2\text{-}SMe)_2$ and $Li_2Me_2Si(NC_6H_4\text{-}2\text{-}SPh)_2$ were obtained as analytically pure samples. For the crystallization of the diethyl ether adducts the lithiation of $Me_2Si(NH\text{-}C_6H_4\text{-}2\text{-}SR)_2$ (R = Me, Ph) was carried out in diethyl ether and afterwards the solutions were layered with *n*-hexane to precipitate **4a** and **5a**. $Li_2Me_2Si(NC_6H_4\text{-}2\text{-}S^tBu)_2$ as precipitated from the *n*-hexane reaction solution contained small amounts of *n*-hexane. Solvent-free samples of **6** were obtained by recrystallization from toluene or diethyl ether.

$Li_2Me_2Si(NC_6H_4\text{-}2\text{-}SMe)_2$ (4)

Yield: 1.49 g (86 %), $C_{16}H_{20}Li_2N_2S_2Si$ (346.44 g/mol), Analysis Li found 3.72 % (calc. 4.00 %)

IR: 3064(w), 3047(w), 2990(w), 2945(w), 2919(w), 1572(s), 1547(w), 1478(m), 1452(s), 1434(s), 1398(w), 1375(w), 1291(m), 1257(s), 1227(s), 1161(w), 1131(m), 1058(m), 1039(m), 956(w), 904(s), 895(s), 837(w), 811(s), 758/s), 721(m), 682(m), 599(s), 557(w), 479(s), 445(m), 411(m), 397(w), 362(m), 329(w), 257(s).

^{1}H NMR (THF-D_8): δ 0.37 (s br, 6H; SiCH_3), 2.08 (s br, 6H; SCH_3), 5.98-6.89 (m, phenylene).

^{13}C NMR (THF-D_8): δ 3.2 (SiCH_3), 19.5 (SCH_3), 110.4, 120.7 (*C*S), 121.6, 127.7, 132.4, 163.2 (*C*N).

^{29}Si NMR (THF-D_8): δ −20.4 (s).

$Li_2Me_2Si(NC_6H_4\text{-}2\text{-}SPh)_2$ (5)

Yield: 2.19 g (93 %), $C_{26}H_{24}Li_2N_2S_2Si$ (470.58 g/mol), Analysis Li found 2.82 % (calc. 2.95 %)

IR: 3084(w), 3069(w), 3057(w), 3046(w), 2954(w), 1577(s), 1539(w), 1476(s), 1450(s), 1425(s), 1375(m), 1286(s), 1261(m), 1236(s), 1180(w), 1163(m), 1128(m), 1070(w), 1051(m), 1030(m), 997(w), 913(s), 838(m), 806(s), 753(s), 731(s), 689(s), 665(m), 595(s), 555(w), 502(s), 482(s), 470(s), 429(s), 385(m), 342(m), 314(w), 287(s), 260(m).

^{1}H-NMR (THF-D_8) (**5a**) : δ 0.02 (s, 6H; SiCH_3),7.20–5.81 (m, phenyl and phenylene H).

^{13}C NMR (THF-D_8): δ 1.4 (SiCH_3), 109.0, 115.2 (*C*-S(phenylene)), 122.9, 124.6, 127.2, 128.9, 130.6, 137.6, 141.8 (*C*-S(Ph)), 166.5 (*C*N).

^{29}Si NMR (THF–D8): δ −21.9

$Li_2Me_2Si(NC_6H_4\text{-}2\text{-}S^tBu)_2$ (6)

Yield: 0.69 g, 0.35 g after recrystallization from diethyl ether (48 %), Analysis Li found 3.25 % (calc. 3.22 %).

IR 2954(w), 2925(w), 2897(w), 2861(w), 1573(m),1477(m), 1447(s),1422(m), 1363(w), 1302(w), 1276(m), 1256(m), 1228(s), 1157(m), 1125(w), 1052(w), 1034(w), 908(s), 813(m), 799(m), 753(s), 731(m), 685(w), 662(w), 601(m), 568(m), 495(m), 440(m), 406(w), 359(w), 327(w), 312(w), 279(m), 237(s).

^{1}H-NMR (THF-D_8): δ 0.01 (SiCH_3), 1.29 (C(CH_3)$_3$), 5.74–7.05 (m, phenylene).

^{13}C NMR (THF-D_8): δ 3.0 (SiCH_3), 32.2 (C(CH_3)$_3$), 48.3 (*C*(CH_3)$_3$), 108.4, 117.4 (*CS*), 123.9, 130.7, 140.3, 168.1 (*CN*).

^{29}Si NMR (THF-D_8): δ −24.8.

Crystal structure refinements

The structures were solved with SHELXT[19] and refined against F^2 with SHELXL[20] using OLEX2 as graphical interface.[21] All hydrogen atoms have been placed at calculated positions riding on their parent atoms with displacement parameters U_{iso}(H) = 1.5 U_{eq}(C) for methyl groups and U_{iso}(H) = 1.2 U_{eq}(C) for the remaining H atoms. Compounds **5** and **4a** were refined with the SQUEEZE routine due to heavily distorted solvate molecules.[22] Graphical representations of the crystal structures were created with the Diamond program.[23]

DFT calculations

DFT calculations were carried out with the Gaussian16 (Rev. C.01) program[24] employing the B3LYP hybrid functional[25] with the def2tzvp[26] basis set. The optimized minima for **4a**–**4c** were confirmed by the absence of imaginary vibrational frequencies.

Acknowledgements

We thank Andreas Kiowski for technical support. Open Access funding enabled and organized by Projekt DEAL.

Conflict of Interest

The authors declare no conflict of interest.

Data Availability Statement

The data that support the findings of this study are available from the corresponding author upon reasonable request.

Keywords: Lithium · Silylamide · X-Ray · Crystal Structure

[1] M. Lappert, P. Power, A. Protechenko, A. Seeber, *Metal Amide Chemistry*, Wiley, **2009**.
[2] V. Passarelli, F. Benetollo, P. Zanella, *Eur. J. Inorg. Chem.* **2004**, 1714.
[3] P. Liebing, K. Merzweiler, *Z. Anorg. Allg. Chem.* **2022**, *648*, e2021003.
[4] P. Liebing, K. Merzweiler, *Z. Anorg. Allg. Chem.* **2017**, *643*, 1220.
[5] R. Albrecht, P. Liebing, U. Morgenstern, C. Wagner, K. Merzweiler, *Z. Naturforsch. B* **2019**, *74*, 233.
[6] U. Morgenstern, C. Wagner, K. Merzweiler, *Z. Anorg. Allg. Chem.* **2019**, *645*, 1.
[7] D. J. Brauer, H. Burger, G. R. Liewald, *J. Organomet. Chem.* **1986**, *308*, 119.
[8] Hong Chen, R. A. Bartlett, H. V. R. Dias, M. M. Olmstead, P. P. Power, *Inorg. Chem.* **1991**, *30*, 2487.
[9] A. Mommertz, R. Leo, W. Massa, K. Harms, K. Dehnicke, *Z. Anorg. Allg. Chem.* **1998**, *624*, 1647.
[10] M. S. Hill, P. B. Hitchcock, *Organometallics* **2002**, *21*, 3258.
[11] Junsheng Hao, Xuehong Wei, Shuping Huang, Jianping Guo, Diansheng Liu, *Appl. Organomet. Chem.* **2005**, *19*, 1010.
[12] S. D. Cosham, A. L. Johnson, G. Kociok-Kohn, K. C. Molloy, *J. Organomet. Chem.* **2014**, *772*, 27.
[13] G. Bendt, D. Blaser, C. Wolper, S. Schulz, **2020**, *CSD Communication*, Refcode IGIHOY.
[14] C. Jones, P. C. Junk, N. A. Smithies, *J. Organomet. Chem.* **2000**, *607*, 105.
[15] B.-D. Lechner, S. Hahn, C. Wagner, K. Merzweiler, *Z. Anorg. Allg. Chem.* **2013**, *639*, 2597.
[16] P. Liebing, K. Merzweiler, *Z. Anorg. Allg. Chem.* **2016**, *642*, 500.
[17] F. H. Allen, *Acta Crystallogr. Sect. B* **2002**, *58*, 380
[18] R. G. Pearson, *J. Am. Chem. Soc.* **1963**, *85*, 3533.
[19] G. M. Sheldrick, *Acta Crystallogr.* **2015**, *A71*, 3.
[20] G. M. Sheldrick, *Acta Crystallogr.* **2015**, *C71*, 3.
[21] O. V. Dolomanov, L. J. Bourhis, R. J. Gildea, J. A. K. Howard, H. Puschmann, *J. Appl. Crystallogr.* **2009**, *42*, 339.
[22] A. Spek, *J. Appl. Crystallogr.* **2003**, *36*, 7.
[23] G. Bergerhoff, K. Brandenburg, *Visual Crystal Structure Information System*, Diamond, Bonn (1996).
[24] Gaussian 16, Revision B.01, M. J. Frisch, G. W. Trucks, H. B. Schlegel, G. E. Scuseria,M. A. Robb, J. R. Cheeseman, G. Scalmani, V. Barone, G. A. Petersson, H. Nakatsuji, X. Li, M. Caricato, A. V. Marenich, J. Bloino, B. G. Janesko, R. Gomperts, B. Mennucci, H. P. Hratchian, J. V. Ortiz, A. F. Izmaylov, J. L. Sonnenberg, D. Williams-Young, F. Ding, F. Lipparini, F. Egidi, J. Goings, B. Peng, A. Petrone, T. Henderson, D. Ranasinghe, V. G. Zakrzewski, J. Gao, N. Rega, G. Zheng, W. Liang, M. Hada, M. Ehara, K. Toyota, R. Fukuda, J. Hasegawa, M. Ishida, T. Nakajima, Y. Honda, O. Kitao, H. Nakai, T. Vreven, K. Throssell, J. A. Montgomery, Jr., J. E. Peralta, F. Ogliaro, M. J. Bearpark, J. J. Heyd, E. N. Brothers, K. N. Kudin, V. N. Staroverov, T. A. Keith, R. Kobayashi, J. Normand, K. Raghavachari, A. P. Rendell, J. C. Burant, S. S. Iyengar, J. Tomasi, M. Cossi, J. M. Millam, M. Klene, C. Adamo, R. Cammi, J. W. Ochterski, R. L. Martin, K. Morokuma, O. Farkas, J. B. Foresman, and D. J. Fox, Gaussian, Inc., Wallingford CT, 2016.
[25] a) A. D. Becke, *J. Chem. Phys.* **1993**, *98*, 5648; b) C. T. Lee, W. T. Yang, R. G. Parr, *Phys. Rev. B* **1988**, *37*, 785.
[26] a) F. Weigend, R. Ahlrichs, *Phys. Chem. Chem. Phys.* **2005**, *7*, 3297; b) F. Weigend, *Phys. Chem. Chem. Phys.* **2006**, *8*, 1057.

Manuscript received: May 12, 2023
Revised manuscript received: July 11, 2023
Accepted manuscript online: July 19, 2023

